

The Extremely Red, Young L Dwarf PSO J318.5338–22.8603: A Free-Floating Planetary-Mass Analog to Directly Imaged Young Gas-Giant Planets

Michael C. Liu^{1,2}, Eugene A. Magnier¹, Niall R. Deacon³, Katelyn N. Allers⁴, Trent J. Dupuy⁵, Michael C. Kotson¹, Kimberly M. Aller¹, W. S. Burgett¹, K. C. Chambers¹, P. W. Draper⁶, K. W. Hodapp¹, R. Jedicke¹, N. Kaiser¹, R.-P. Kudritzki¹, N. Metcalfe⁶, J. S. Morgan¹, P. A. Price⁷, J. L. Tonry¹, R. J. Wainscoat¹

ABSTRACT

We have discovered using Pan-STARRS1 an extremely red late-L dwarf, which has $(J - K)_{MKO} = 2.84$ and $(J - K)_{2MASS} = 2.78$, making it the reddest known field dwarf and second only to 2MASS J1207–39b among substellar companions. Near-IR spectroscopy shows a spectral type of $L7 \pm 1$ and reveals a triangular H -band continuum and weak alkali (K I and Na I) lines, hallmarks of low surface gravity. Near-IR astrometry from the Hawaii Infrared Parallax Program gives a distance of 24.6 ± 1.4 pc and indicates a much fainter J -band absolute magnitude than field L dwarfs. The position and kinematics of PSO J318.5–22 point to membership in the β Pic moving group. Evolutionary models give a temperature of 1160^{+30}_{-40} K and a mass of $6.5^{+1.3}_{-1.0} M_{\text{Jup}}$, making PSO J318.5–22 one of the lowest mass free-floating objects in the solar neighborhood. This object adds to the growing list of low-gravity field L dwarfs and is the first to be strongly deficient in methane relative to its estimated temperature. Comparing their spectra suggests that young L dwarfs with similar ages and temperatures can have different spectral signatures of youth. For the two objects with well constrained ages (PSO J318.5–22 and 2MASS J0355+11), we find their temperatures are ≈ 400 K cooler than field objects of similar spectral type but their luminosities are comparable, i.e.,

¹Institute for Astronomy, University of Hawaii, 2680 Woodlawn Drive, Honolulu HI 96822

²Visiting Astronomer at the Infrared Telescope Facility, which is operated by the University of Hawaii under Cooperative Agreement no. NNX-08AE38A with the National Aeronautics and Space Administration, Science Mission Directorate, Planetary Astronomy Program.

³Max Planck Institute for Astronomy, Konigstuhl 17, D-69117 Heidelberg, Germany

⁴Department of Physics and Astronomy, Bucknell University, Lewisburg, PA 17837

⁵Hubble Fellow. Harvard-Smithsonian Center for Astrophysics, 60 Garden Street, Cambridge, MA 02138

⁶Department of Physics, Durham University, South Road, Durham DH1 3LE, UK

⁷Department of Astrophysical Sciences, Princeton University, Princeton, NJ 08544, USA

these young L dwarfs are very red and unusually cool but not “underluminous.” Altogether, PSO J318.5–22 is the first free-floating object with the colors, magnitudes, spectrum, luminosity, and mass that overlap the young dusty planets around HR 8799 and 2MASS J1207–39.

Subject headings: brown dwarfs — parallaxes — planets and satellites: atmospheres — proper motions — solar neighborhood — surveys

1. Introduction

A major surprise arising from direct detection of gas-giant planets around young stars is that the spectral properties of these objects differ from those of field L and T dwarfs (e.g. Chauvin et al. 2005; Marois et al. 2008; Bowler et al. 2010; Patience et al. 2010; Barman et al. 2011a; Bowler et al. 2013). These young planets have redder near-IR colors, fainter near-IR absolute magnitudes, and peculiar spectra compared to their field analogs. Over the last several years, this development has fostered closer scrutiny of the long-standing paradigm that a simple physical sequence connects the lowest mass stars to brown dwarfs to gas-giant planets.

We now know that most field brown dwarfs are not good analogs to young exoplanets. In contrast to field T dwarfs of similar temperature, the young planets around HR 8799 and 2MASS J1207–39 have no methane absorption and very red colors. These properties are thought to arise from extreme atmospheric conditions tied to their young (≈ 10 – 30 Myr) ages and low gravities, e.g., enhanced vertical mixing, non-equilibrium chemistry, and unusual clouds (e.g. Barman et al. 2011b; Madhusudhan et al. 2011; Marley et al. 2012). This is corroborated by recent studies of the youngest (~ 10 – 100 Myr) field brown dwarfs, which find that low-gravity L dwarfs also show very red colors and spectral peculiarities (e.g. McLean et al. 2003; Kirkpatrick et al. 2008). Complicating this interpretation, however, is the existence of very red L dwarfs that do not show spectral signatures of youth (e.g. Kirkpatrick et al. 2010; Allers & Liu 2013). Thus, similarities between the colors and spectra of field brown dwarfs and young planets can have ambiguous interpretations.

There are two prominent shortfalls in our observational knowledge. (1) There are only a handful of very red young L dwarfs currently known (see compilation in Gizis et al. 2012), and only one of them has a parallax measurement (Faherty et al. 2013; Liu et al. 2013). (2) Most L dwarfs do not have as red near-IR colors as young exoplanets, and *none* are as faint in their near-IR absolute magnitudes. Therefore, the utility of young field objects as exoplanet analogs may be limited, since the existing samples of these two types of objects are small and do not really overlap.

We have found an extraordinary young L dwarf that will help shed light on these topics. It is the reddest field object found to date and the first to have absolute magnitudes comparable to directly imaged young dusty exoplanets.

2. Observations

We have been undertaking a search for T dwarfs using the Pan-STARRS1 (PS1) 3π Survey (Deacon et al. 2011; Liu et al. 2011). We select objects using Pan-STARRS1 and 2MASS based on their colors and proper motions and then obtain near-infrared photometry for further screening. We observed PSO J318.5338–22.8603 (hereinafter PSO J318.5–22) using WFCAM on the UK Infrared Telescope (UKIRT) on the 2010 September 15 UT. Conditions were photometric with 0.9–1.0'' seeing. We found that the $(J - K)_{MKO}$ color for PSO J318.5–22 was 2.74 ± 0.04 mag (Table 1), significantly redder than any previously known field dwarf.

We obtained $R \approx 100$ near-IR (0.8–2.5 μm) spectra on 2011 July 21 UT from NASA’s Infrared Telescope Facility. (By coincidence, we observed PSO J318.5–22 immediately before obtaining the spectrum of the similarly red L dwarf WISE J0047+68 published in Gizis et al. 2012.) Conditions were photometric with 1'' seeing. We used the near-IR spectrograph SpeX (Rayner et al. 1998) in prism mode with the 0.8'' slit. The total on-source integration time was 16 min. All spectra were reduced using version 3.4 of the SpeXtool software (Vacca et al. 2003; Cushing et al. 2004). We also used the final spectrum to synthesize near-IR colors for PSO J318.5–22 (Table 1).

To assess the gravity of PSO J318.5–22, we obtained $R \approx 1700$ near-IR spectra using the GNIRS spectrograph (Elias et al. 2006) on the Gemini-North 8.1-m Telescope. Cross-dispersed spectra were obtained using the 0.3'' slit and the 32 lines mm^{-1} grating on the nights of 2013 June 26, June 30, and July 01 UT. The total integration time was 5400 s. We reduced the data using a version of SpeXtool modified for GNIRS cross-dispersed data. We combined the telluric-corrected spectra from the three nights using a robust weighted mean to produce the final 0.95–2.5 μm spectrum.

We conducted astrometric monitoring of PSO J318.5–22 with the facility near-IR camera WIRCam at the Canada-France-Hawaii Telescope, obtaining 9 epochs over 2.0 years starting on 2011 July 26 UT. Our methods are described in Dupuy & Liu (2012). Using 116 reference stars in the field of PSO J318.5–22, the resulting median astrometric precision per epoch was 4.0 mas, and the best-fit proper motion and parallax solution had $\chi^2 = 13.2$ with 13 degrees of freedom. We applied a relative-to-absolute parallax correction of 0.74 ± 0.13 mas derived from the Besançon model of the Galaxy (Robin et al. 2003). Table 1 gives our astrometry results. We did not find any objects co-moving with PSO J318.5–22 in our $10'.4 \times 10'.4$ field of view within a range between 0.6 mag fainter and 3.3 mag brighter at J band.

3. Results

3.1. Spectrophotometric Properties

The colors of PSO J318.5–22 are extreme, with $(J - K)_{MKO} = 2.78$ mag, $(J - K)_{2MASS} = 2.84$ mag, and $(W1 - W2) = 0.76 \pm 0.04$ mag, all being the reddest among field L dwarfs (Figure 1 and also

see Gizis et al. 2012). Such colors are thought to arise from an unusually dusty atmosphere that results from a low surface gravity (young age). The position of PSO J318.5–22 on the near-IR color-magnitude diagram is similarly extreme, being significantly fainter in J -band absolute magnitude than field L dwarfs (Figure 1). It coincides with the colors and magnitudes of the directly imaged planets around HR 8799 and 2MASS J1207–39b.

We determine the near-IR spectral type of PSO J318.5–22 using the Allers & Liu (2013) system, which provides gravity-insensitive types consistent with optical spectral types. For late-L dwarfs, visual classification in the J and K bands and index-based classifications with the H₂OD index are applicable. For the GNIRS spectrum of PSO J318.5–22, we visually assign a J -band type of L9±1 and a K -band type of L6±1. The H₂OD index corresponds to L6.0±0.8. The weighted mean of these three determinations leads to a final type of L7±1. Spectral typing of our low-resolution SpeX spectrum gives the same classification (Table 1).

PSO J318.5–22 shows a triangular H -band continuum, which is considered a hallmark of youth (e.g. Lucas et al. 2001). However, Allers & Liu (2013) caution that very red L-dwarfs having no signatures of youth (low gravity) can display a triangular H -band shape (e.g., 2MASS J2148+40 in Figure 2). At moderate resolution, there are other indicators of youth for late-L dwarfs. Our GNIRS spectrum displays a weak 1.20 μm FeH band as well as weak Na I (1.14 μm) and K I (1.17 and 1.25 μm) lines, which indicate a low gravity. Using the gravity-sensitive indices of Allers & Liu (2013), we classify PSO J318.5–22 as VL-G, which Allers & Liu suggest correspond to ages of \sim 10–30 Myr based on the (small) sample of young late-M/early-L dwarfs with good age constraints. Altogether, PSO J318.5–22 visually appears most similar to the red L dwarfs WISE J0047+68 (Gizis et al. 2012) and 2MASS J2244+20 (McLean et al. 2003), in accord with the similar spectral types and gravity classifications for these three objects.

Allers & Liu (2013) note that objects of the same age and spectral type (temperature) can display different spectral signatures of youth, based on 2 young L dwarfs in the AB Dor moving group. Our new discovery affirms this idea. The spectra of 2MASS J1207–39b and PSO J318.5–22 are quite different (Figure 2), despite their similar colors and absolute magnitudes and the fact they may be coeval (Section 3.2). PSO J318.5–22 shows a negative continuum slope from 2.12–2.28 μm , whereas 2MASS J1207–39b has a positive slope. The H -band continuum of PSO J318.5–22 displays a “shoulder” at 1.58 μm , whereas 2MASS J1207–39b has a very peaked continuum. Overall, the spectrum of 2MASS J1207–39b appears most similar to that of 2MASS J0355+11 (both objects have near-IR types of L3 VL-G), despite their large differences in ages, colors, and absolute magnitudes. Altogether, these comparisons hint that determining relative ages and temperatures from NIR spectra may be unexpectedly complex.

To assess the physical parameters, we fit the low-resolution near-IR spectra of PSO J318.5–22 and 2MASS J0355+11 with the Ames/DUSTY model atmospheres (Allard et al. 2001) and the BT-Settl model atmospheres (Allard et al. 2011) with two different assumed solar abundances (Asplund et al. 2009 [AGSS] and Caffau et al. 2011 [CIFIST]). Since both objects have parallaxes,

the scaling factors (R^2/d^2) from the fits provide an estimate of the objects’ radii. Using χ^2 minimization, all three sets of models indicates that PSO J318.5–22 ($T_{\text{eff},\text{atm}} = 1400 - 1600 \text{ K}$) is 100–200 K cooler than 2MASS J0355+11 ($T_{\text{eff},\text{atm}} = 1600 - 1700 \text{ K}$). BT-Settl/AGSS models give the best fits, with the resulting temperatures being comparable to previous fitting of field L dwarfs but with both young objects having lower surface gravities ($\log(g)=4.0\text{--}4.5 \text{ dex}$) than field objects (Cushing et al. 2008; Stephens et al. 2009; Testi 2009, though the number of fitted field objects is small). Most strikingly, the fitted radii are implausibly small ($\approx 0.8 R_{\text{Jup}}$), indicating discord between the data and models even though the quality of fit seems adequate by eye. A similar radius mismatch occurs in model atmosphere fitting of young dusty planets (e.g., Bowler et al. 2010; Barman et al. 2011a; cf., Marley et al. 2012).

3.2. Group Membership

There is no radial velocity (RV) for PSO J318.5–22, but we can place modest constraints on its space motion. Published RVs (Blake et al. 2010; Seifahrt et al. 2010; Rice et al. 2010; Shkolnik et al. 2012) find that low-gravity late-M and L dwarfs reside in the range of $[-20, +25] \text{ km s}^{-1}$, with the smaller RV range compared to field objects being expected given the young ages. Figure 3 plots the spatial (XYZ) and kinematic (UVW) location of PSO J318.5–22 compared to the young moving groups (YMGs) from Torres et al. (2008).¹ Its XYZ position is coincident with the β Pic, Tuc-Hor, and AB Dor moving groups. However, the velocity information makes the Tuc-Hor and AB Dor groups implausible, given the large offset from PSO J318.5–22. Overall, the match with the β Pic members is excellent, i.e., the velocity offset between the group and PSO J318.5–22 would be only 3 km s^{-1} if PSO J318.5–22 has an RV of -6 km s^{-1} .

We also computed the kinematic distance (d_{kin}) and angle θ from Schlieder et al. (2010). d_{kin} is an object’s distance assuming that its tangential velocity (as derived from its observed proper motion) is the same as the mean tangential velocity of a YMG. Including the uncertainties in the β Pic group’s UVW , PSO J318.5–22 has $d_{\text{kin}} = 20.8_{-1.0}^{+1.1} \text{ pc}$, in good agreement with its parallactic distance. θ gives the angle between the object’s proper motion and that of the YMG at the object’s sky position. PSO J318.5–22 has $\theta = 8_{-5}^{+4}$, whereas the β Pic members from Torres et al. (2008) mostly have $\theta < 15 \text{ degs}$. In other words, for PSO J318.5–22 the amplitude and direction of its tangential velocity given its sky location agrees well with the space motion of known β Pic members.

Finally, we computed the YMG membership probability using the online calculator of Malo et al. (2013). Given the position and parallax of PSO J318.5–22, their Bayesian method reports a membership probability of 99.9% in the β Pic YMG and 0.01% in the field. (Removing the parallax as an input, their method gives 99.6% and a predicted distance of $22.5 \pm 1.6 \text{ pc}$, in good agreement

¹ U and X are positive toward the Galactic Center, V and Y are positive toward the direction of galactic rotation, and W and Z are positive toward the North Galactic Pole.

with our parallactic distance.) The absolute value of this method’s probabilities is imperfect, since their input model for the solar neighborhood does not account for the relative numbers of objects in different YMGs and the field. However, the high probability for PSO J318.5–22 is comparable to the values computed for most of the known β Pic members (and exceeds the rest of them). The Malo et al. method also does not consider the fact that PSO J318.5–22 is spectroscopically young, which would boost the probability that it is a YMG member rather than a field object (since most field objects have old ages).

3.3. Physical Properties

PSO J318.5–22, 2MASS J0355+11, and 2MASS J1207–39b are all moving group members and thus play an important role as “age benchmarks” (e.g. Pinfield et al. 2006; Liu et al. 2008) for very red L dwarfs. With a measured L_{bol} and an age estimate, we use the Saumon & Marley (2008) evolutionary models with $f_{\text{sed}} = 2$ to compute the remaining physical properties. (Results from the other commonly available evolutionary models are similar, comparable to the uncertainties.)

To derive L_{bol} , we combined our 0.9–2.4 μm low-resolution spectra flux-calibrated using the *JHK* photometry, the *WISE* *W1* and *W2* photometry, and the best-fitting atmospheric model (Section 3.1) for the flux at bluer and redder wavelengths. We integrated the fluxes and used the parallaxes to determine L_{bol} , with the uncertainties in the input data (spectra, photometry, and parallax) handled in a Monte Carlo fashion. We find $\log(L_{\text{bol}}/L_{\odot}) = -4.42 \pm 0.06$ dex and -4.23 ± 0.11 dex for PSO J318.5–22 and 2MASS J0355+11, respectively, very similar to field mid/late-L dwarfs (Golimowski et al. 2004; Cushing et al. 2006). Young, very red L dwarfs are sometimes (and confusingly) described as “underluminous” compared to field objects, but we find that the luminosities of young and old field objects are comparable.² Rather, these objects have fainter absolute magnitudes in the bluer near-IR bands (e.g., *J* band) but comparable L_{bol} ’s. They are therefore better described as being “very red.”

For PSO J318.5–22, using an age of 12_{-4}^{+8} Myr (distributed uniformly) from Zuckerman et al. (2001), we find a mass of $6.5_{-1.0}^{+1.3} M_{\text{Jup}}$, temperature of 1160_{-40}^{+30} K, and $\log(g)$ of $3.86_{-0.08}^{+0.10}$ dex (Figure 4). Adopting a larger age range of 10–100 Myr (distributed uniformly), the mass becomes $12 \pm 3 M_{\text{Jup}}$, with T_{eff} and $\log(g)$ increasing only slightly (Table 1). Such cool temperatures correspond to a field $\approx T5.5$ dwarf (Golimowski et al. 2004) and yet PSO J318.5–22 shows no sign of CH_4 in its spectrum, similar to the situation for the planets around HR 8799 and 2MASS J1207–39. (e.g. Marois et al. 2008; Bowler et al. 2010; Patience et al. 2010; Barman et al. 2011a). The evolutionary-model radii are almost twice as large as those from our model atmosphere fits, as has previously been noted in analysis of directly imaged planets (Section 3.1).

²Note that 2MASS J1207–39b can be described as “underluminous,” as its luminosity ($\log(L_{\text{bol}}/L_{\odot}) = -4.73 \pm 0.12$ dex; Barman et al. 2011b) is somewhat low relative to field L dwarfs.

Our same calculations for 2MASS J0355+11 give a mass of $24_{-6}^{+3} M_{\text{Jup}}$, temperature of 1420_{-130}^{+80} K, and $\log(g)$ of $4.58_{-0.17}^{+0.07}$ dex, assuming an age of 125 ± 25 Myr (Barenfeld et al. 2013) based on its membership in the AB Dor moving group (Faherty et al. 2013; Liu et al. 2013). This object is more massive and hotter than PSO J318.5–22, as expected given its brighter absolute magnitudes and older age. Faherty et al. (2013) describe 2MASS J0355+11 as having a strong resemblance to a giant exoplanet. While it does have similar H and K -band spectra to 2MASS J1207–39b (but not in J band nor the overall SED shape; Figure 2), 2MASS J0355+11 is ≈ 2 mag brighter in J band (Figure 1) and $\approx 5 \times$ more massive than 2MASS J1207–39b. Likewise, the spectrum of HR 8799b has been shown to resemble some field dwarfs (e.g., 2MASS J2148+40 and 2MASS J2244+20 by Bowler et al. 2010 and 2MASS J2139+02 by Barman et al. 2011a), yet HR 8799b is much fainter and lower mass. This strengthens our finding that *near-IR spectral morphology can not reliably determine the underlying physical properties of very red young objects.*

The temperatures for these two objects are substantially lower than those measured in the same fashion (using L_{bol} , age, and evolutionary models) for field L dwarfs of comparable spectral types. Golimowski et al. (2004) find T_{eff} of 1700–1950 K for spectral types L3–L5 (corresponding to the near-IR and optical types for 2MASS J0355+11) and 1500 K for L7 (the near-IR type for PSO J318.5–22). Thus, the temperatures of these young, very red L dwarfs are ≈ 400 K cooler than comparable field objects. Bowler et al. (2013) show that young L-type companions tend to have cooler temperatures than (old) field objects of the same type. Our results show that this offset also occurs for young free-floating objects.

4. Discussion

PSO J318.5–22 shares a strong physical similarity to the young dusty planets HR 8799bcd and 2MASS J1207–39b, as seen in its colors, absolute magnitudes, spectrum, luminosity, and mass. Most notably, it is the first field L dwarf with near-IR absolute magnitudes as faint as the HR 8799 and 2MASS J1207–39 planets, *demonstrating that the very red, faint region of the near-IR color-magnitude diagram is not exclusive to young exoplanets.* Its probable membership in the β Pic moving group makes it a new substellar benchmark at young ages and planetary masses. We find very red, low-gravity L dwarfs have ≈ 400 K cooler temperatures relative to field objects of comparable spectral type, yet have similar luminosities. Comparing very red L dwarf spectra to each other and to directly imaged planets highlights the challenges of diagnosing physical properties from near-IR spectra.

PSO J318.5–22 is among the lowest-mass free-floating objects identified in the solar neighborhood. Dupuy & Kraus (2013) have determined parallaxes and luminosities of field Y dwarfs and thereby estimate masses of 7–20 M_{Jup} , assuming ages of 1–5 Gyr. The (likely Y dwarf) companion WD 0806–661B has a precise age from its white dwarf primary, leading to a mass of 6–10 M_{Jup} (Luhman et al. 2012; Dupuy & Kraus 2013). Delorme et al. (2012) have identified a candidate young late-T dwarf member of the AB Dor moving group with an estimated mass of 4–7 M_{Jup} ,

though a parallax and RV are needed to better determine its properties and membership (and thus age and mass).

PSO J318.5–22 was not discovered by previous large-area searches for L dwarfs using 2MASS (Reid et al. 2008; Cruz et al. 2003). PSO J318.5–22 has only tenuous detections in the 2MASS J and H bands, and the resulting colors lie outside the selection criteria of Cruz et al. (2003). Additionally, the object is too far south to be detected by SDSS, and it is not in the areas surveyed so far by UKIDSS or VISTA. However, both the PS1 and VISTA datasets are growing relative to what has been searched here, both in depth and area, and upcoming surveys (e.g., LSST) will have even greater reach. Thus, wide-field surveys mapping the whole sky offer a promising avenue for understanding exoplanets directly imaged in the tiny areas around the brightest stars.

The Pan-STARRS1 surveys have been made possible by the Institute for Astronomy, the University of Hawaii, the Pan-STARRS Project Office, the institutions of the Pan-STARRS1 Science Consortium (<http://www.ps1sc.org>), NSF, and NASA. We thank Brendan Bowler for assistance with the figures and Michael Cushing for providing a pre-release update of SpeXtool. Our research has employed the *WISE* and 2MASS data products; NASA’s Astrophysical Data System; and the Spex Prism Spectral Libraries maintained by Adam Burgasser. This research was supported by NSF grants AST09-09222 (awarded to MCL) and AST-0709460 (awarded to EAM) as well as AFRL Cooperative Agreement FA9451-06-2-0338. Finally, the authors wish to recognize and acknowledge the very significant cultural role and reverence that the summit of Mauna Kea has always had within the indigenous Hawaiian community. We are most fortunate to have the opportunity to conduct observations from this mountain.

Facilities: IRTF (SpeX), CFHT (WIRCAM)

REFERENCES

- Allard, F., Hauschildt, P. H., Alexander, D. R., Tamanai, A., & Schweitzer, A. 2001, *ApJ*, 556, 357
- Allard, F., Homeier, D., & Freytag, B. 2011, in *Astronomical Society of the Pacific Conference Series*, Vol. 448, 16th Cambridge Workshop on Cool Stars, Stellar Systems, and the Sun, ed. C. Johns-Krull, M. K. Browning, & A. A. West, 91
- Allers, K. N., & Liu, M. C. 2013, *ApJ*, 772, 79
- Asplund, M., Grevesse, N., Sauval, A. J., & Scott, P. 2009, *ARA&A*, 47, 481
- Barenfeld, S. A., Bubar, E. J., Mamajek, E. E., & Young, P. A. 2013, *ApJ*, 766, 6
- Barman, T. S., Macintosh, B., Konopacky, Q. M., & Marois, C. 2011a, *ApJ*, 733, 65
- . 2011b, *ApJ*, 735, L39
- Best, W. M. J., et al. 2013, *ArXiv e-prints*
- Biller, B. A., et al. 2013, *ArXiv e-prints*
- Blake, C. H., Charbonneau, D., & White, R. J. 2010, *ApJ*, 723, 684
- Bowler, B. P., Liu, M. C., Dupuy, T. J., & Cushing, M. C. 2010, *ApJ*, 723, 850
- Bowler, B. P., Liu, M. C., Shkolnik, E. L., & Dupuy, T. J. 2013, *ApJ*, 774, 55
- Caffau, E., Ludwig, H.-G., Steffen, M., Freytag, B., & Bonifacio, P. 2011, *Sol. Phys.*, 268, 255
- Chauvin, G., Lagrange, A.-M., Dumas, C., Zuckerman, B., Mouillet, D., Song, I., Beuzit, J.-L., & Lowrance, P. 2005, *A&A*, 438, L25
- Cruz, K. L., Reid, I. N., Liebert, J., Kirkpatrick, J. D., & Lowrance, P. J. 2003, *AJ*, 126, 2421
- Cushing, M. C., et al. 2008, *ApJ*, 678, 1372
- Cushing, M. C., Vacca, W. D., & Rayner, J. T. 2004, *PASP*, 116, 362
- Cushing, M. C., et al. 2006, *ApJ*, 648, 614
- Deacon, N. R., et al. 2011, *AJ*, 142, 77
- Delorme, P., et al. 2012, *A&A*, 548, A26
- Dupuy, T. J., & Kraus, A. L. 2013, *ArXiv e-prints*
- Dupuy, T. J., & Liu, M. C. 2012, *ApJS*, 201, 19

- Elias, J. H., Joyce, R. R., Liang, M., Muller, G. P., Hileman, E. A., & George, J. R. 2006, in Society of Photo-Optical Instrumentation Engineers (SPIE) Conference Series, Vol. 6269, Society of Photo-Optical Instrumentation Engineers (SPIE) Conference Series
- Faherty, J. K., Rice, E. L., Cruz, K. L., Mamajek, E. E., & Núñez, A. 2013, *AJ*, 145, 2
- Gizis, J. E., et al. 2012, *AJ*, 144, 94
- Golimowski, D. A., et al. 2004, *AJ*, 127, 3516
- Kirkpatrick, J. D., et al. 2008, *ApJ*, 689, 1295
- . 2010, *ApJS*, 190, 100
- Kuzuhara, M., et al. 2013, *ApJ*, 774, 11
- Leggett, S. K., et al. 2010, *ApJ*, 710, 1627
- Liu, M. C., Dupuy, T. J., & Allers, K. N. 2013, *Astronomische Nachrichten*, 334, 85
- Liu, M. C., Dupuy, T. J., & Ireland, M. J. 2008, *ApJ*, 689, 436
- Liu, M. C., et al. 2011, *ApJ*, 740, L32
- Looper, D. L., et al. 2008, *ApJ*, 686, 528
- Lucas, P. W., Roche, P. F., Allard, F., & Hauschildt, P. H. 2001, *MNRAS*, 326, 695
- Luhman, K. L., et al. 2012, *ApJ*, 744, 135
- Madhusudhan, N., Burrows, A., & Currie, T. 2011, *ApJ*, 737, 34
- Malo, L., Doyon, R., Lafrenière, D., Artigau, É., Gagné, J., Baron, F., & Riedel, A. 2013, *ApJ*, 762, 88
- Marley, M. S., Saumon, D., Cushing, M., Ackerman, A. S., Fortney, J. J., & Freedman, R. 2012, *ApJ*, 754, 135
- Marois, C., Macintosh, B., Barman, T., Zuckerman, B., Song, I., Patience, J., Lafrenière, D., & Doyon, R. 2008, *Science*, 322, 1348
- McLean, I. S., McGovern, M. R., Burgasser, A. J., Kirkpatrick, J. D., Prato, L., & Kim, S. S. 2003, *ApJ*, 596, 561
- Patience, J., King, R. R., de Rosa, R. J., & Marois, C. 2010, *A&A*, 517, A76
- Pinfield, D. J., Jones, H. R. A., Lucas, P. W., Kendall, T. R., Folkes, S. L., Day-Jones, A. C., Chappelle, R. J., & Steele, I. A. 2006, *MNRAS*, 368, 1281

- Rayner, J. T., Toomey, D. W., Onaka, P. M., Denault, A. J., Stahlberger, W. E., Watanabe, D. Y., & Wang, S. 1998, in *Proc. SPIE: Infrared Astronomical Instrumentation*, ed. A. M. Fowler, Vol. 3354, 468–479
- Reid, I. N., Cruz, K. L., Kirkpatrick, J. D., Allen, P. R., Mungall, F., Liebert, J., Lowrance, P., & Sweet, A. 2008, *AJ*, 136, 1290
- Rice, E. L., Barman, T., Mclean, I. S., Prato, L., & Kirkpatrick, J. D. 2010, *ApJS*, 186, 63
- Robin, A. C., Reylé, C., Derrière, S., & Picaud, S. 2003, *A&A*, 409, 523
- Saumon, D., & Marley, M. S. 2008, *ApJ*, 689, 1327
- Schlieder, J. E., Lépine, S., & Simon, M. 2010, *AJ*, 140, 119
- Seifahrt, A., Reiners, A., Almaghrbi, K. A. M., & Basri, G. 2010, *A&A*, 512, A37
- Shkolnik, E. L., Anglada-Escudé, G., Liu, M. C., Bowler, B. P., Weinberger, A. J., Boss, A. P., Reid, I. N., & Tamura, M. 2012, *ApJ*, 758, 56
- Stephens, D. C., et al. 2009, *ApJ*, 702, 154
- Testi, L. 2009, *A&A*, 503, 639
- Torres, C. A. O., Quast, G. R., Melo, C. H. F., & Sterzik, M. F. 2008, *Young Nearby Loose Associations*, ed. Reipurth, B., 757
- Vacca, W. D., Cushing, M. C., & Rayner, J. T. 2003, *PASP*, 115, 389
- Zuckerman, B., Song, I., Bessell, M. S., & Webb, R. A. 2001, *ApJ*, 562, L87

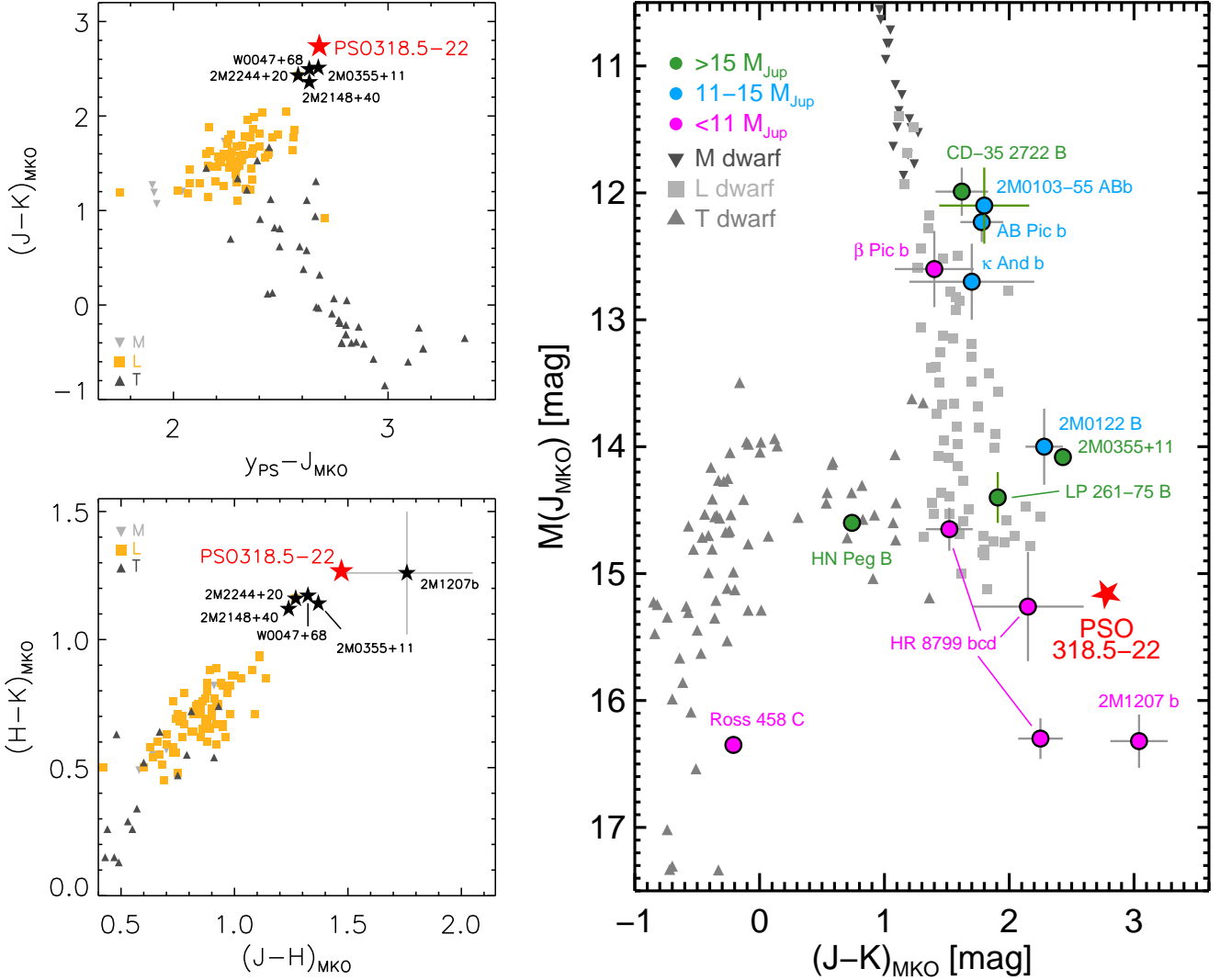


Fig. 1.— **Left:** Color-color diagrams using optical+IR (*top left*) and IR-only (*bottom left*) photometry. Field objects are plotted based on our PS1 photometry (y_{P1}) and the MKO photometry (JHK) compilation by Leggett et al. (2010). The extreme colors of PSO J318.5–22 compared to the field population are evident. Also shown are the young planetary-mass object 2MASS 1207–39b (Chauvin et al 2005) and the very red field L dwarfs 2MASS J2148+40, 2MASS J2244+20, 2MASS J0355+11, and WISE J0047+68. **Right:** PSO J318.5–22 compared to known substellar objects based on the compilations of Dupuy & Liu (2012), Bowler et al. (2013), and references therein. Young substellar companions are highlighted, with the AB Pic b data from Biller et al. (2013). PSO J318.5–22 is very red and faint compared to field L dwarfs, with magnitudes and colors comparable to the planets around HR 8799 and 2MASS J1207–39. (Its measurements uncertainties are smaller than the symbol size.)

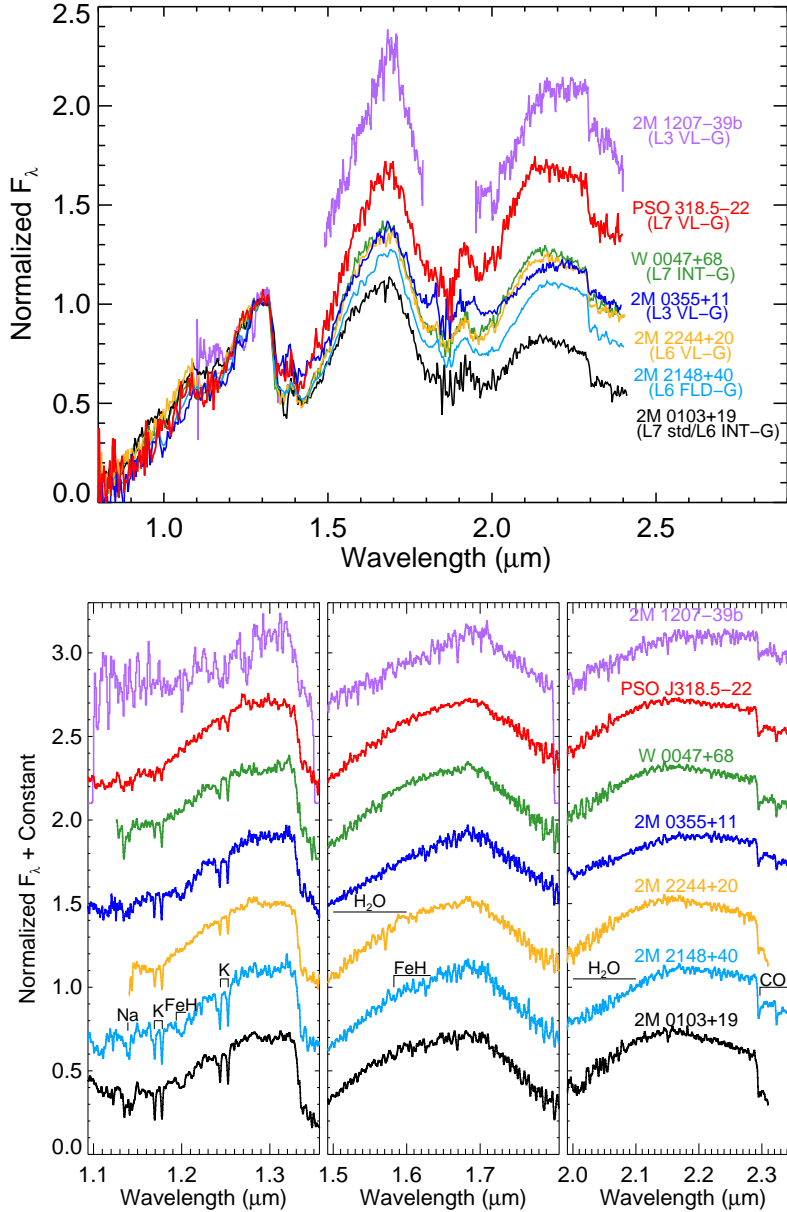


Fig. 2.— Spectrum of PSO J318.5–22 compared to the L7 near-IR standard 2MASS J0103+19 of Kirkpatrick et al. (2010); the dusty field object 2MASS J2148+40 (Looper et al. 2008, which we classify as L6±1 FLD-G); the L6 VL-G standard 2MASS J2244+20 from Allers & Liu (2013); the very red L dwarfs 2MASS J0355+11 (Reid et al. 2008; Faherty et al. 2013; Allers & Liu 2013) and WISE J0047+68 (Gizis et al. 2012; Gizis et al., in prep.); and the young planetary-mass object 2MASS 1207–39b (Patience et al. 2010). The labels use near-IR types and gravity classifications on the Allers & Liu system, except for the Kirkpatrick et al. (2010) L7 standard (which Allers & Liu classify as L6 INT-G in the near-IR). **Top:** Low-resolution ($R \approx 100$) spectra, normalized to the J -band peak (1.26–1.31 μm). The 2MASS J1207–39b spectrum has been lightly smoothed. Note that despite having similar colors, luminosities, and ages, 2MASS J1207–39b and PSO J318.5–22 have very different H -band continuum shapes. **Bottom:** Moderate-resolution spectra for the same young and/or dusty objects, all smoothed to $R = 750$. The weaker J -band Na I and K I lines for PSO J318.5–22 compared to 2MASS J2244+20 and WISE J0047+68 indicate a lower gravity.

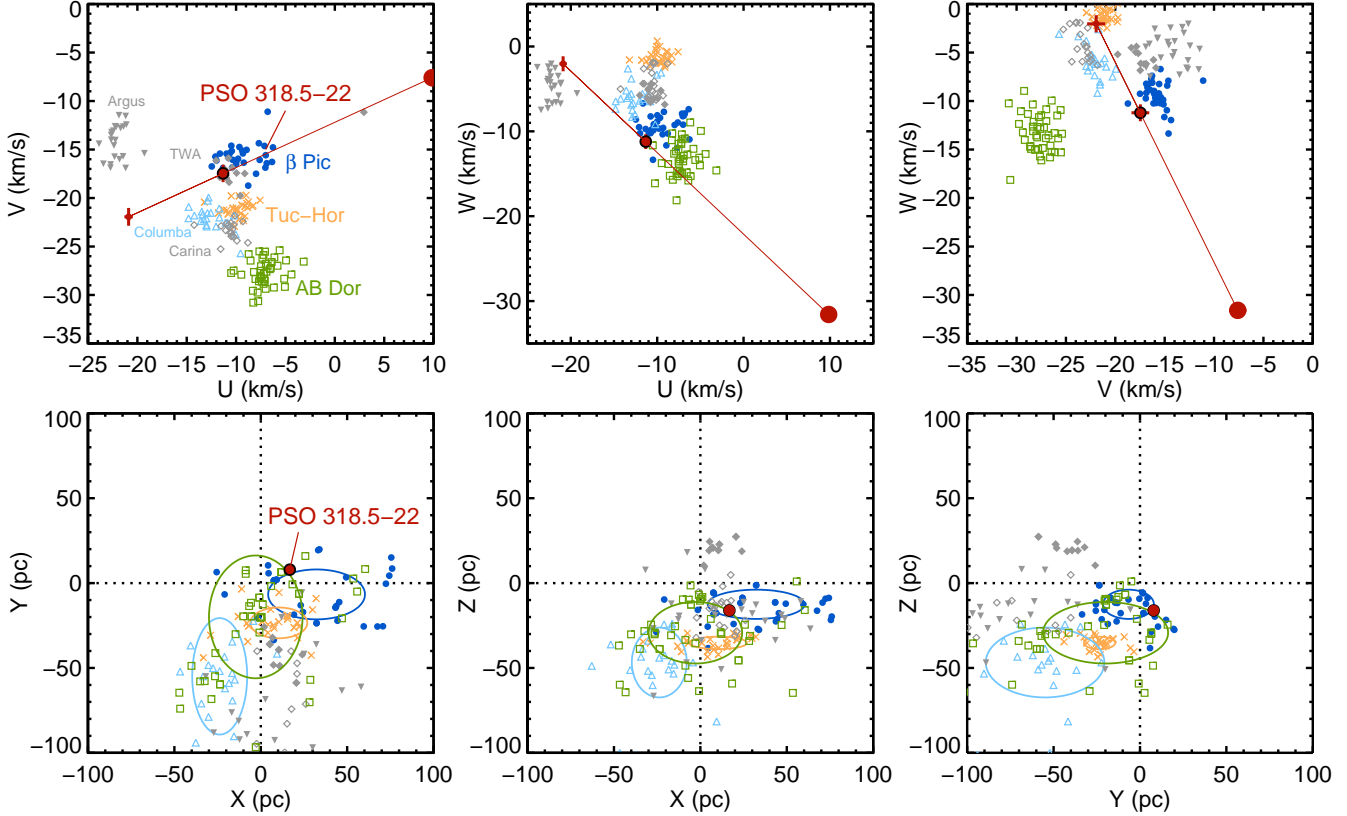


Fig. 3.— Kinematic and spatial position of PSO J318.5–22 (red circle) compared to known YMGs from Torres et al. (2008). For the UVW plots, we adopt an RV of $[-20, +25]$ km s^{-1} (Section 3.2), with the larger red circles being more positive velocities and the red line being the full RV range. Uncertainties arising from errors in the distance and proper motion (but not the RV) are shown at the 3 red circles. The members of the nearest YMGs to PSO J318.5–22 are shown in color and the others in grey, with the ellipses representing the RMS of the known members. Consideration of both the XYZ and UVW data indicate the β Pic group is the only possibility. The middle (black-outlined) circle shows the UVW position of PSO J318.5–22 for an RV of -6 km s^{-1} .

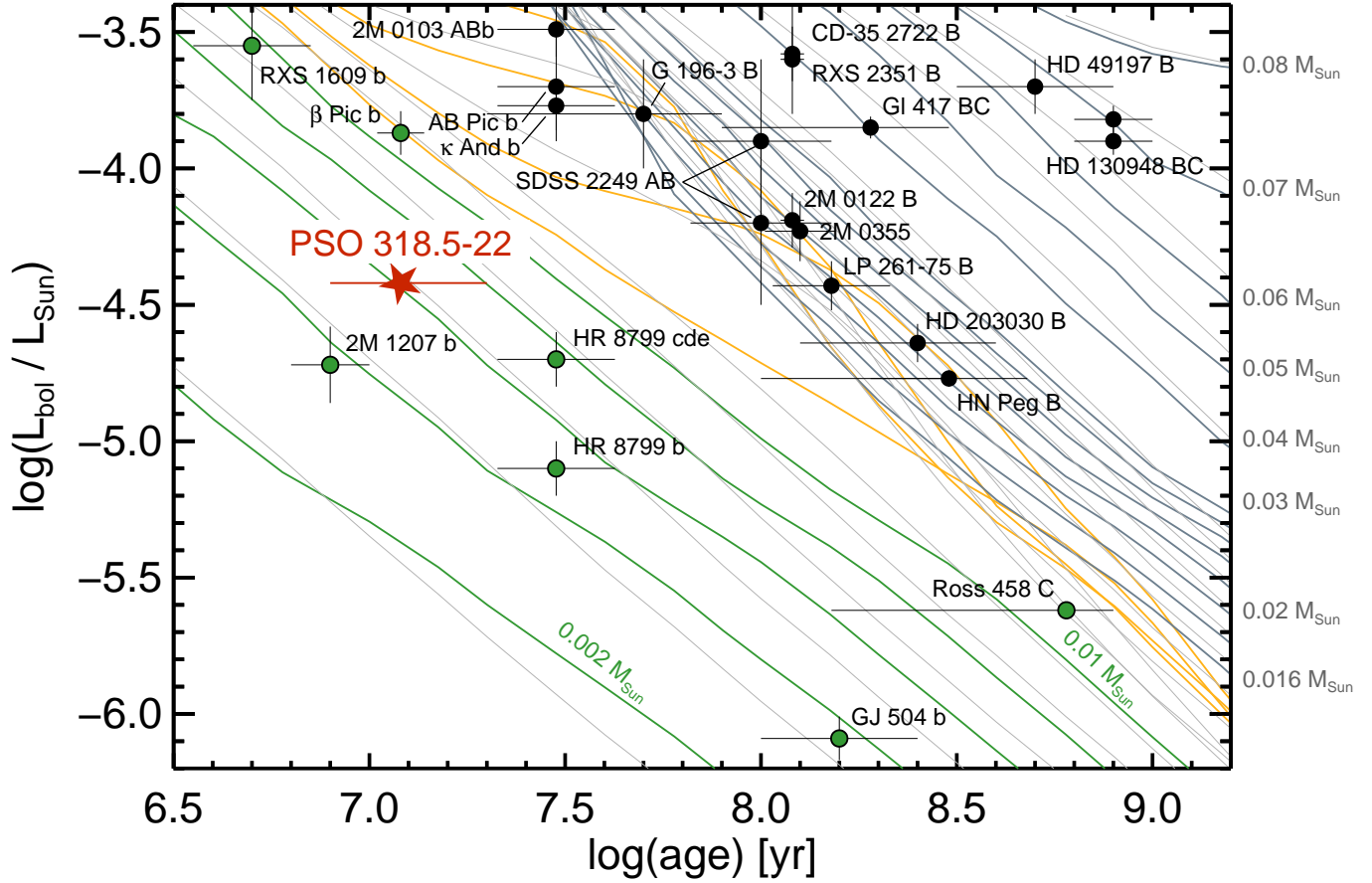


Fig. 4.— PSO J318.5–22 and known young substellar objects from Kuzuhara et al. (2013) and the compilation of Bowler et al. (2013). The Saumon & Marley (2008) cloudless evolutionary models are plotted in color, with 0.002–0.010 M_{\odot} tracks in green (spaced by 0.002 M_{\odot}), 0.011–0.014 M_{\odot} tracks in yellow (where D-burning may complicate the interpretation and spaced by 0.001 M_{\odot}), and $\geq 0.016 M_{\odot}$ in grey (spaced by 0.002 M_{\odot} up to 0.030 M_{\odot} and then by 0.010 M_{\odot}). The thin light grey lines show the cloudy evolutionary models with $f_{sed} = 2$.

Table 1. Measurements of PSO J318.5338–22.8603

Property	Measurement
Nomenclature	
2MASS	2MASS J21140802–2251358
Pan-STARRS1	PSO J318.5338–22.8603
WISE	WISE J211408.13–225137.3
Astrometry (Equinox J2000)	
2MASS RA, Dec (ep 1999.34)	318.53344, –22.85996
Pan-STARRS1 RA, Dec (ep 2010.0)	318.53380, –22.86032
WISE RA, Dec (ep 2010.34)	318.53388, –22.86037
Proper motion μ_α, μ_δ (mas/yr)	$137.3 \pm 1.3, -138.7 \pm 1.4$
Proper motion amplitude μ (″/yr)	195.0 ± 1.3
Proper motion PA (°)	135.3 ± 0.4
Parallax π (mas)	40.7 ± 2.4
Distance d (pc)	24.6 ± 1.4
v_{tan} (km/s)	22.7 ± 1.3
Photometry	
PS1 g_{P1} (AB mag)	$>23.6 (3\sigma)^a$
PS1 r_{P1} (AB mag)	$>23.1 (3\sigma)^a$
PS1 i_{P1} (AB mag)	$>22.9 (3\sigma)^a$
PS1 z_{P1} (AB mag)	20.80 ± 0.09^a
PS1 y_{P1} (AB mag)	19.51 ± 0.07^a
2MASS J (mag)	16.71 ± 0.20
2MASS H (mag)	15.72 ± 0.17
2MASS K_S (mag)	14.74 ± 0.12
MKO Y (mag)	18.81 ± 0.10
MKO J (mag)	17.15 ± 0.04
MKO H (mag)	15.68 ± 0.02
MKO K (mag)	14.41 ± 0.02
WISE $W1$ (mag)	13.22 ± 0.03
WISE $W2$ (mag)	12.46 ± 0.03
WISE $W3$ (mag)	11.8 ± 0.4
WISE $W4$ (mag)	$>8.6 (2\sigma)$

Table 1—Continued

Property	Measurement
Synthetic photometry ^b	
2MASS $J - H$ (mag)	1.678 ± 0.007 (0.06)
2MASS $H - K_S$ (mag)	1.159 ± 0.004 (0.03)
2MASS $J - K_S$ (mag)	2.837 ± 0.006 (0.07)
MKO $Y - J$ (mag)	1.37 ± 0.02 (0.05)
MKO $J - H$ (mag)	1.495 ± 0.007 (0.06)
MKO $H - K$ (mag)	1.279 ± 0.004 (0.03)
MKO $J - K$ (mag)	2.775 ± 0.007 (0.07)
$(J_{2MASS} - J_{MKO})$ (mag)	0.111 ± 0.002
$(H_{2MASS} - H_{MKO})$ (mag)	-0.072 ± 0.001
$(K_{S,2MASS} - K_{MKO})$ (mag)	0.049 ± 0.001
$\log(L_{\text{bol}}/L_{\odot})$ (dex)	-4.42 ± 0.06
Spectral classification ^c	
J -band type (SpeX, GNIRS)	$L8 \pm 1, L9 \pm 1$
H -band type (SpeX, GNIRS)	$L6 \pm 1, L6 \pm 1$
$H_2\text{OD}$ type (SpeX, GNIRS)	$L6.0 \pm 0.9, L6.0 \pm 0.8$
Gravity score (SpeX, GNIRS)	XXX2, 2X21
Final near-IR spectral type	$L7 \pm 1$
Near-IR gravity class	VL-G
Physical Properties (age = 12^{+8}_{-4} Myr)	
Mass (M_{Jup})	6.5 ($-1.0, +1.3$)
$T_{\text{eff,evol}}$ (K)	1160 ($-40, +30$)
$\log(g_{\text{evol}})$ (cgs)	3.86 ($-0.08, +0.10$)
Radius (R_{Jup})	1.53 ($-0.03, +0.02$)
Physical Properties (age = 10–100 Myr)	
Mass (M_{Jup})	12 ± 3
$T_{\text{eff,evol}}$ (K)	1210 ($-50, +40$)
$\log(g_{\text{evol}})$ (cgs)	4.21 ($-0.16, +0.11$)
Radius (R_{Jup})	1.40 ($-0.04, +0.06$)

^aAverage of multi-epoch photometry. The optical non-detections are consistent with the colors of late-L dwarfs ($i_{P1} - z_{P1} \approx 2.0 - 2.5$ mag; Best et al. 2013).

^bColors were synthesized from our SpeX spectrum, with formal errors derived from the spectrum’s measurement errors. The values in parentheses are the estimated systematic errors, calculated from comparing the measured JHK colors for ~ 100 objects to the colors synthesized from the SpeX Prism Library. This additional uncertainty is needed to reconcile the two sets of results such that $P(\chi^2) \approx 0.5$. No systematic errors ($\lesssim 0.02$ mag) were measurable for the 2MASS-to-MKO conversion within a given bandpass (Dupuy & Liu 2012).

^cBased on the classification system of Allers & Liu (2013).